

Two-Phase Flow Patterns in Large Diameter Vertical Pipes at High Pressures

N. K. Omebere-Iyari and B. J. Azzopardi

Multiphase Flow Research Group, Nottingham Fuel and Energy Centre, School of Chemical, Environmental and Mining Engineering, The University of Nottingham, University Park, Nottingham NG7 2RD, U.K.

Y. Ladam

Wellstream Technology, SINTEF Petroleum Research, NO-7465 Trondheim, Norway

DOI 10.1002/aic.11288

Published online August 28, 2007 in Wiley InterScience (www.interscience.wiley.com).

The flow pattern characteristics for a mixture of naphtha and nitrogen in a 52-m high, 189-mm diameter vertical pipe at 20 and 90 bar are reported. Time varying, void fraction and pressure variations along the riser were measured. For the former, gamma densitometers were employed. It was found that the classic slug flow pattern was not present in these experiments. The observed flow patterns are classified as bubble, intermittent, semiannular, and annular. All the methods for flow pattern transitions in vertical two-phase flow tested against the present experiments give poor predictions. The identification and delineation of flow patterns using probability density function distribution of the cross-sectionally averaged void fraction is consistent with the methods of employing pressure gradient fluctuations and structure velocity. © 2007 American Institute of Chemical Engineers AICHE J, 53: 2493–2504, 2007

Keywords: two-phase flow, flow pattern transitions, void fraction, large diameter, vertical pipe

Introduction

Typically, in offshore exploration of oil and gas, steeply inclined riser pipelines link the seabed system to the floating production vessel. With fields being developed in ever increasing water depths, the importance of large diameter vertical and steeply inclined riser systems to limit the pressure drop is increasing. New field developments such as Girassol (operated by TotalFinaElf) and Roncador (Petrobras) are about 1300- and 1500- to 2000-m deep, respectively. The limitation of available data to diameters much smaller than those typical of field applications provides severe challenges to the methodologies derived from work on smaller diameter

pipes for predicting flow pattern, phase fraction (hold-up), and pressure gradient. This is because current evidence suggests that flow patterns and other parameters are different in small and large pipes.

There is very little work available in large diameter vertical pipes. Hills,¹ Hashemi et al.,² Kytomaa and Bremen,³ and Cheng et al.⁴ are a few of the researchers to have worked with such pipes. The results of studies seeking the bubble/slug transition of air–water flows in a 150-mm diameter pipe by Cheng et al.⁴ indicated that over the ranges of flow rates where slug flow would normally appear, no conventional large bubbles occupying the majority of the pipe cross section were seen except under transient conditions such as start-up. This was contrary to previous investigations by many researchers. For example, Taitel et al.⁵ and Costigan and Whalley,⁶ with pipes of smaller diameters seem to suggest that gas–liquid two-phase flow in vertical pipes exhibits bubble, slug, churn, and annular flows with the increase of void fraction. Cheng et al.⁴ concluded that instead

Current address of N. K. Omebere-Iyari: Granherne Ltd., Kellogg, Brown and Root (KBR), Leatherhead KT22 7LH, U.K.

Correspondence concerning this article should be addressed to B. J. Azzopardi at barry.azzopardi@nottingham.ac.uk.

of traditional slug flow in their column, there is a very gradual transition to a type of churn flow as the gas rate is increased. However, they found that the void fraction fluctuated periodically. This was observed in the signals of cross-sectionally averaged void fraction and point void fraction probes and is a behavior associated with intermittent flows. Ohnuki and Akimoto⁷ investigated upward air-water two-phase flow in a large diameter pipe (200 mm) and reported that churn flow is dominant in the large diameter pipe under the conditions where small-scale pipes have slug flow. Based on observations through the transparent pipe wall they classified the flow patterns observed as undisturbed bubbly, agitated bubbly, churn bubbly, churn slug, and churn froth. This type of observations are difficult and what is seen is biased by the bubbles or film near the wall. Ohnuki and Akimoto⁷ also reported radial profiles of time averaged velocities, void fraction, and bubble sizes. Though these profiles can distinguish between the wall peak and centre peak types of bubbly flows, they are not so useful at discriminating between other flow patterns. In one of their figures, Ohnuki and Akimoto show radial void fraction profiles from their 200-mm pipe for a run that they identify as churn flow and from a smaller (25 mm) pipe in which the run is slug flow. There is nothing to distinguish the profiles. Some confirmation of the flow patterns suggested by Ohnuki and Akimoto is provided by work at Rossendorf, Germany using their mesh electrode system as described in the papers of Prasser et al.⁸ They could produce virtual side projections for air/water in a 194-mm pipe. These are integrated versions given a view as would be seen through a transparent pipe wall. It is not so easy to discriminate flow patterns from this view. However, projections of the data from across a diameter show support for the flow patterns suggested by Ohnuki and Akimoto. In experiments performed by Kobayashi et al.,⁹ ideally shaped Taylor bubbles were absent and the observed flow patterns were similar to those obtained by Ohnuki and Akimoto.⁷ Kytomaa and Brennen³ in their work with air and water in a 102-mm diameter column, found a transition from bubbly flow to churn-turbulent rather than to slug. There exists therefore, a strong possibility that slug flow does not actually exist in large diameter pipes in the form envisaged by the most commonly used flow pattern maps. Later work¹⁰⁻¹² corroborates the absence of conventional slug flows in large diameter pipes.

Hills et al.¹³ reanalyzed the data of Cheng et al.⁴ and found that the time series data from local void fraction probes and those from cross-sectionally averaging probes showed the same characteristic frequency.

The material published to date on gas/liquid flow in large diameter vertical pipes has been on air and water at near atmospheric pressure. To appreciate the effect of gas density, liquid viscosity, and surface tension it is possible to draw on the extensive literature on bubble columns. These units operate with zero or very small liquid velocity. Research has been published on columns of 0.1- to 1-m diameter but with lengths of 1-4 m. A major observation is that at low gas rates, the flow consists of small bubbles uniformly dispersed about the column. This is normally called homogeneous flow. It differs from the usage of this word in gas/liquid flow in pipes where equal gas and liquid velocity are implied. In bubble columns it implies well dispersed small bubbles. At

higher gas velocities larger bubbles which are interspersed between the small ones appear. This is termed the heterogeneous regime as all extra gas is believed to go into the large bubbles. The gradient of void fraction with gas superficial velocity is smaller in the heterogeneous regime than in the homogeneous regime. Though much of the work has been carried out with water, some papers¹⁴⁻¹⁶ present data for organic liquids which show a slightly higher void fraction than for water. The effect of gas density has been studied by using: (i) different gases¹⁴ and (ii) increase of pressure.¹⁷ This increase in the gas density increases the void fraction but the effect peters off at about a value of 10 kg/m³. The effect of mixtures was examined using water with alcohols^{18,19} or sodium sulphate²⁰ or with mixtures of organic chemicals.²⁰ The effect of the additive is to increase void fraction but the void fraction/gas superficial velocity gradient in the heterogeneous regime is lower than that for the pure substance. In both cases (increase in gas density and the addition of additives), the increase in void fraction is believed to be due to a movement of the homogeneous/heterogeneous transition point. The general consensus is that the effect of additives achieves this by inhibiting coalescence of bubbles. This is supported by work which has measured bubble sizes.²⁰ Letzel et al.¹⁷ produced a model to predict the void fraction which provides separate equations involving many empirical constants for the small and large bubble void fractions. These are then combined. The papers cited above are not the only ones covering this material but are exemplars.

In this article, time varying void fraction and pressure gradient data have been obtained for a two-phase mixture of nitrogen and naphtha at high pressures in the 189-mm diameter, 52-m high vertical riser of the SINTEF Multiphase Flow laboratory in Norway. The results have been analyzed for the purpose of establishing and delineating the extant flow patterns and their transitions. Comparisons have been made with the most common prediction methods for flow patterns and improved flow pattern transitions for our conditions are presented.

Prediction Methods for Flow Pattern Transitions

Radovcich and Moissis²¹ attributed the bubble-to-slug transition to collisions between small bubbles, some of which results in coalescence, producing bubbles that are similar in diameter to the tube and characteristic of slug flow. Bubbly flow is thus a transient and intermediate flow regime, which, after a long enough residence time in a pipe, will develop into slug flow. Taitel et al.⁵ were in agreement with the claim that gradual bubble coalescence is responsible for the transition. An increase in gas rate corresponds to an increase in bubble density which results in a greater rate of coalescence. At higher liquid flow rates, the bubbles formed as a result of agglomeration can be broken up by turbulent fluctuations. This dispersed bubble pattern can be maintained if the break-up intensity is sufficient to prevent recoalescence. However, at liquid rates low enough so that bubble break-up due to turbulence is small, the number of collisions increases and a there is sharp rise in the agglomeration to larger bubbles. It is only by this mechanism that discrete bubbles com-

Table 1. Physical Properties of Nitrogen and Naphtha

Pressure (bar)	Temperature (°C)	Density		Viscosity		Surface Tension (N/m)
		Gas (kg/m ³)	Liquid (kg/m ³)	Gas (Pa s)	Liquid (Pa s)	
20	30	23.4	702.3	1.77E-05	3.59E-04	0.0185
90	30	102.5	700.5	1.93E-05	3.25E-04	0.0134

bine into the larger vapor spaces, with a diameter approximately equal to the tube. Taitel et al.⁵ proposed that this occurs as the void fraction reaches 0.25 and results in a transition to slug flow.

Based on an extensive literature search, Jayanti and Hewitt²² identified four major and different mechanisms for the transition from slug to churn flow. These are entrance mechanism,^{5,23} flooding mechanism,²⁴ wake effect mechanism,²⁵ and bubble coalescence mechanism.²⁶ Jayanti and Hewitt²² propose the mechanism of flooding as the most likely cause of the transition from slug to churn flow in vertical tubes. An improvement to the modeling of the flooding mechanism given by McQuillan and Whalley,²⁴ which was capable of predicting the transition over the full range of liquid rates, is also suggested. In the model of Jayanti and Hewitt,²² the empirical correlation of Brotz²⁷ for the film thickness surrounding the Taylor bubble which Fulford²⁸ showed to be applicable over a wide range of film Reynolds numbers, replaced the relationship of Nusselt.²⁹ The second major modification was the incorporation of an empirical correlation to account for the effect of the length of the falling film on the flooding velocity. The model of Jayanti and Hewitt²² was found to give good predictions of the slug-to-churn transition by Watson and Hewitt.³⁰

Barnea^{31,32} developed a model for the transition from annular to intermittent flow, in which the effect of inclination is incorporated. This eliminated the problem of selecting an applicable model for different inclinations, as the transition criteria is the same. The transition from annular to intermittent flow is proposed to occur when the gas core is blocked

at any location by the liquid. There are two mechanisms by which this blockage may occur. The first mechanism which predominates at low liquid flow rates is the instability of the annular configuration. The second mechanism is caused by spontaneous blockage of the gas core as a result of axial transfer of liquid in the film. This instability is a result of the low core shear stress causing the downward flow of the film and blockage of the gas core.

Experimental Arrangement

The experimental facility described by Norris et al.³³ in which the test section encompasses a long horizontal pipeline culminating in a riser, has been modified to introduce the gas and liquid phases at the base of the vertical riser, to minimize upstream effects. The test fluids used were nitrogen and naphtha (a mixture of liquid hydrocarbons) at pressures of 20 and 90 bar and a nominal temperature of 30°C. Table 1 gives the physical properties of nitrogen and naphtha at these conditions. The naphtha is a mixture of 66 hydrocarbon chemicals created to model those liquids produced from wells. It contains molecules with 3 to 25+carbon atoms, is mainly aliphatic but contains ~16% by weight C₆ ring compounds and ~5% C₅ ring compounds. The major components (pentane, hexane, methyl cyclopentane, and cyclohexane) constitutes ~45% by weight.

A simplified schematic diagram of the experimental arrangement is shown in Figure 1. The test section consists

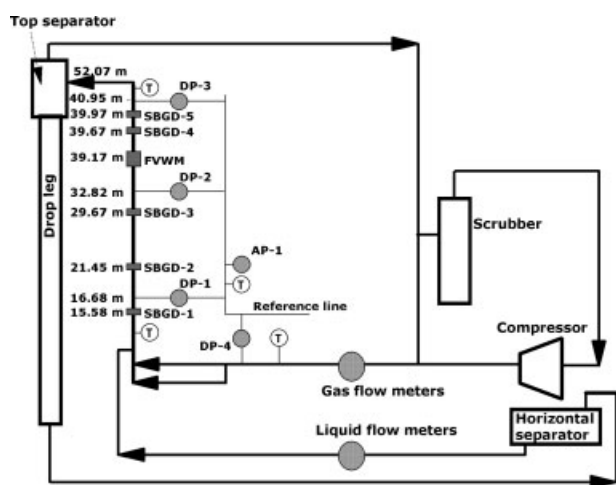


Figure 1. Schematic diagram of the large scale loop rig with the riser test section.

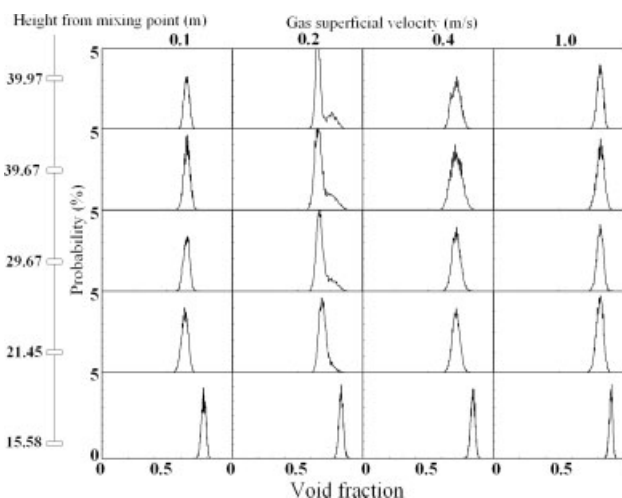
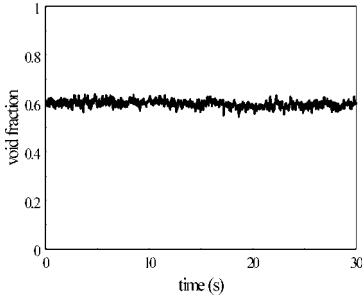
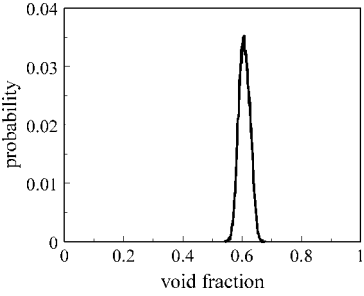
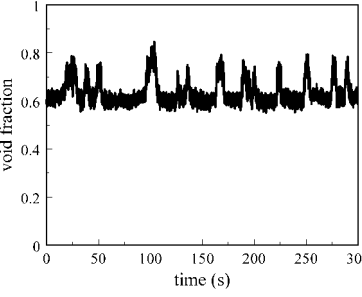
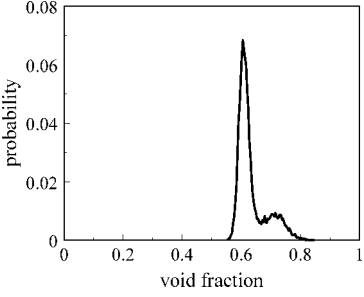
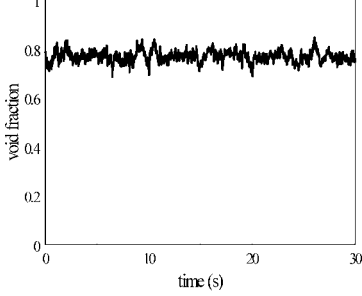
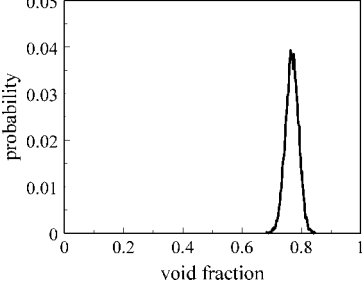
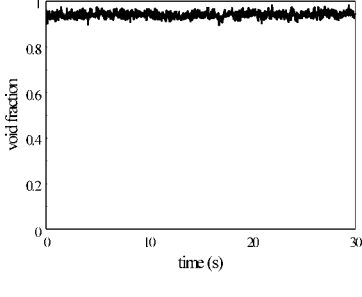
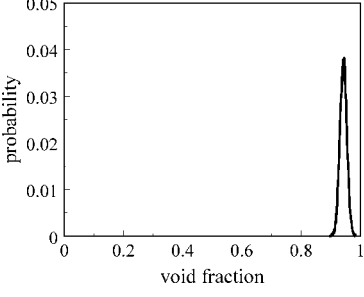


Figure 2. Flow development along the riser test section; liquid superficial velocity of 0.05 m/s and gas superficial velocities of 0.1, 0.2, 0.4, and 1 m/s, respectively.

Table 2. Typical Time Varying, Void Fraction Traces, and Probability Density Function Plots

U_{GS} (m/s)	Time Varying , Void Fraction	Probability Density Function, (PDF)	Flow Pattern
0.1			Bubble
0.21			Intermittent
1.0			Semi annular
4.0			Annular

of a 52-m high riser with an internal pipe diameter of 189 mm. The two-phase flow from the riser enters the top separator where the initial separation occurs. The liquid falls through the drop-leg to the horizontal separator where any residual gases are removed, after which the liquid is transferred to the mixing point using centrifugal pumps. The liquid flow rate was measured by one of four turbine meters. The gas passed through a scrubber to remove any residual

liquid and then recompressed. Its flow rate was measured with one of three vortex flow meters and then is mixed with the liquid phase. In the course of the experiments, three different mixing configurations were used to introduce the gas phase. In one the gas was introduced through 300, 5-mm diameter holes on the inside wall of the annulus through which the liquid flowed and the bubbly mixture entered the main pipe. In the second arrangement the gas entered through a

central pipe and the liquid through an annular gap. In some tests, both methods were used simultaneously.

Gamma densitometers were used to determine time varying, phase fractions in the riser test section. As the gamma rays are attenuated differently in gas and liquid, the radiation intensity at the detector depends on the phase distribution in the pipe. The densitometers employ a Cs 137 radioactive source with a half life of 30.07 years and an original strength of 300 mCi. Two types of gamma instruments have been used: the fast volume weight meter (FVWM) and single beam gamma densitometer (SBGD). The FVWM uses a broad beam to give a cross-sectionally averaged phase fraction while the SBGDs are simpler and use a single beam to yield line fractions which can be used for observing the propagation of structures. The gamma densitometers were subjected to rigorous daily calibration procedures.

The location of the instrumentation along the riser test section is shown in Figure 1. SBGDs were positioned at 82 (15.58 m), 113 (21.45 m), 157 (29.67 m), 210 (39.67 m), and 211 (39.97 m) pipe diameters downstream of the mixing point. Time varying, cross-sectionally averaged void fraction is acquired from the FVWM at a distance of 207 pipe diameters (39.17 m) downstream of the mixer, at which position the flow is expected to have developed. The local pressures in the riser test section are measured by three pairs of sensitive differential pressure transmitters (DP 1-3), which are located at 16.7, 32.8, and 41 m above the mixing point. The transmitters measured the difference in pressure between the two-phase flow line and a nitrogen-filled reference line whose absolute pressure was known. Time varying pressure gradient data is obtained by performing a linear regression analysis of the pressure data from all three measuring positions. Two temperature sensors are located at the top and bottom of the riser. A pressure transducer (DP-4) and temperature sensor are positioned at the gas measurement station so that accurate estimates of the flow in the riser are obtained.

For each experiment, data from the flow meters, gamma densitometers, pressure transducers, and temperature sensors were acquired at 50 Hz for 300 s.

Results and Analysis

Two-phase flow measurements were taken at gas superficial velocities of 0.09 to 14.8 m/s for liquid superficial velocities of 0.004 to 4 m/s at 20 bar and gas superficial velocities of 0.1 to 6 m/s for liquid superficial velocities of 0.004 to 3 m/s at 90 bar.

Flow development

It was observed that the downstream flow characteristics were unaffected by the mixing configuration employed. Probability density function (PDF) plots of the line void fraction measurements obtained from the single beam densitometers at different axial locations were used to describe the flow development along the test section. The representative PDF plots given in Figure 2 are for experiments at 20 bar for a liquid superficial velocity of 0.05 m/s and gas superficial velocities of 0.1, 0.2, 0.4, and 1 m/s.

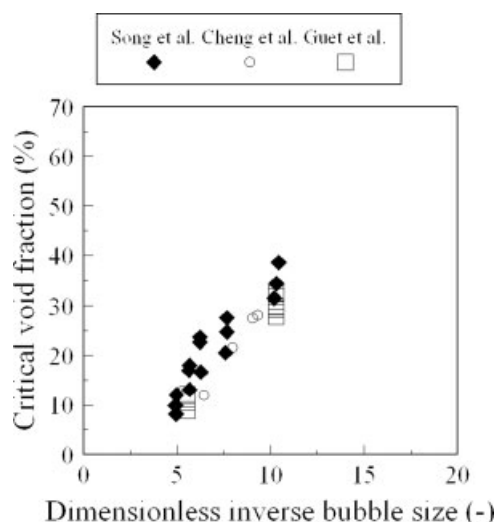


Figure 3. Critical void fraction for various bubble sizes.³⁴

At the first measurement station, the void fraction distributions in all four experiments are characterized by a single peak situated at high void fractions. As expected, the void fraction distribution shifts towards higher values with an increase in the gas superficial velocity. The most profound change between the lowest and highest PDF plots is observed when the gas superficial velocity is 0.2 m/s. Here, the void fraction distribution evolves from a single high void fraction peak to a lower void fraction peak and an elongated tail. This change suggests a transformation in flow pattern along the test section. At gas superficial velocities of 0.1, 0.4, 1.0 m/s, the change in the PDF plots with height is less dramatic, albeit the data at 0.4 m/s possesses a broader PDF distribution. The consistency of the PDF plots between the third and the highest densitometers suggests that the flows can be said to be fully developed from 157 pipe diameters (or 29.7 m) above the riser inlet.

Flow pattern identification

Time varying void fraction traces and their corresponding PDF distributions have been used to identify the observed flow patterns, in a similar manner to Costigan and Whalley.⁶ Typical examples are shown in Table 2 for a liquid superficial velocity of 0.05 m/s at 20 bar. The current flow patterns have been classified as either bubble, intermittent, semiannular, and annular, in contrast to the established bubble, slug, churn, and annular flow patterns in smaller pipes.

Bubble flow is taken to cover both the classic flow pattern in which small bubbles are distributed in a liquid continuum and the churn-turbulent pattern. The PDF distributions are characterized by narrow single peaks. These occur at void fractions of up to 0.7 which is close to the value for maximum packing. The value is also identified in the changes in trends in the variation in pressure gradient intensity discussed below. It also is in line with the trends seen in critical void fraction for bubble/slug transition. Azzopardi³⁴ has gathered data which indicates that where the bubble size is known the critical void fraction is shown to depend on the dimension-

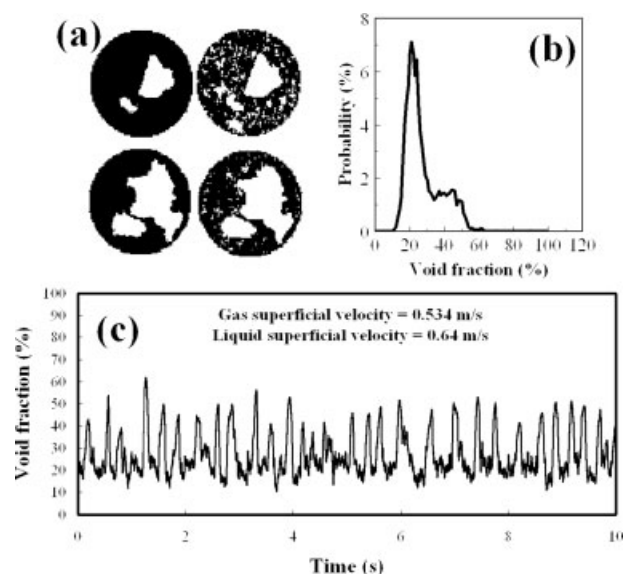


Figure 4. Data for air/water flow in a 194-mm diameter vertical pipe and its visual reconstruction.

(a) Original resolved data: right hand images—complete data; left hand images—large bubbles only; (b) probability density function of (c); (c) time varying cross-sectionally averaged void fraction. Reproduced with the kind permission of H.-M. Prasser, Forschungszentrum Rossendorf, Germany.

less inverse bubble size, i.e., the pipe to bubble diameter ratio. This is reproduced in Figure 3. If typical bubble sizes of 5–15 mm are assumed for the present work, then a critical void fraction of about 0.7 appears possible. It is noted that this is obtained by extrapolation. This value of 0.7 should be contrasted with those used in previous work. In smaller pipe sizes Taitel et al.⁵ and Mishima and Ishii²⁵ propose that the critical void fraction for the transition from bubbly to slug flow is 0.25 and 0.30, respectively. Though Zhu et al.¹² using an air–water mixture in a 200-mm diameter vertical tube quoted a transition at a void fraction of 0.16, this is between bubble and churn-turbulent, a flow pattern transition not present in the current study.

A void fraction of at least 0.85 is taken to signify the onset of annular flow. This value was chosen because it

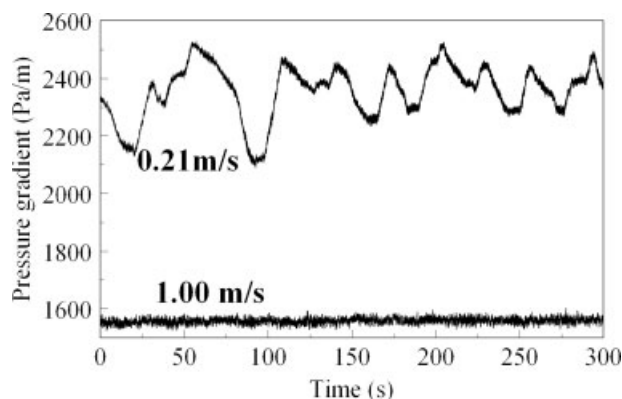


Figure 5. Time varying, pressure gradient for liquid superficial velocity of 0.05 m/s at 20 bar.

Gas superficial velocities: top, 0.21 m/s (intermittent), bottom, 1.0 m/s (semiannular).

agrees with the observation of Costigan and Whalley⁶ that for annular flow their measured void fractions were always above 0.8. The PDF distribution for annular flow consists of a narrow single peak at high void fractions. Though a similar distribution is obtained for void fractions between 0.7 and 0.85, annular flow is linked with void fraction >0.85 because a similar transition is obtained from the trends in structure velocity with mixture velocity discussed below.

The flow pattern showing more pronounced fluctuations in the void fraction traces and where periodic structures are present is referred to as intermittent flow. A feature of the PDF distribution is a “peak and a half” or a broad peak existing between the void fractions of 0.5–0.8. This is unlike the very distinct bi-modal peaks representing the liquid slug and Taylor bubble in slug flow and we do not therefore consider this regime to be slug flow. It is possible that this flow regime contains bubbles not quite approximating to the tube diameter and highly aerated liquid slugs. Notably, none of the void fraction traces represents the oscillatory structure of churn flow which has been previously reported for a wide range of vertical pipes by Omebere-Iyari and Azzopardi³⁵ and Cheng et al.⁴ amongst others in 5- and 150-mm-diameter pipes, respectively.

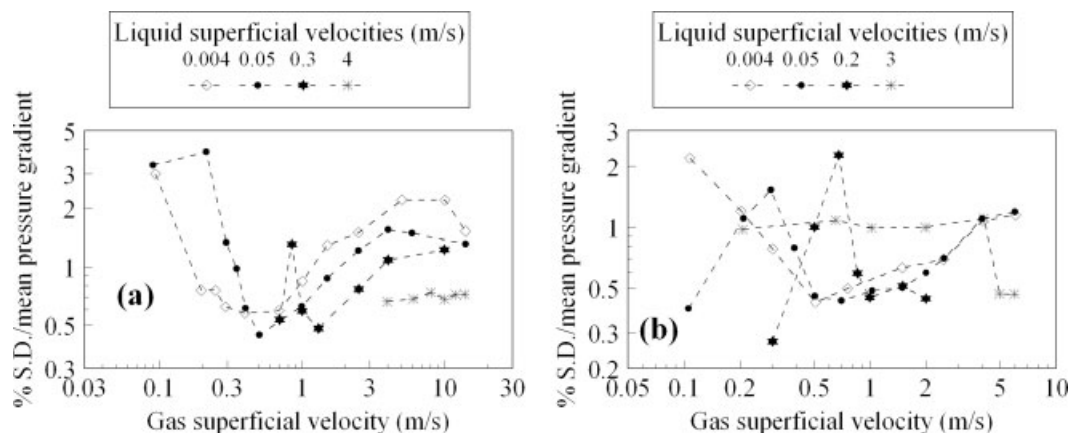


Figure 6. Standard deviation/mean of pressure gradient versus gas superficial velocity at: (a) 20 bar; (b) 90 bar.

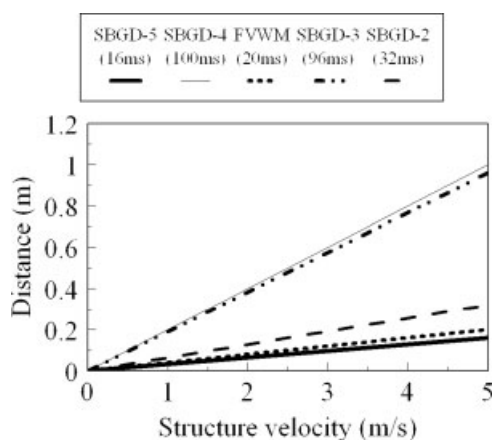


Figure 7. Axial resolution of the gamma densitometers with integration times.

Evidence to support the absence of slug flow can be seen in the cross-sectionally resolved images given in Figure 4. They were obtained using wire mesh sensors for air/water flow in the TOPFLOW facility of Forschungszentrum Rossendorf, in a pipe of similar diameter to the present arrangement. For their time varying, cross-sectionally averaged void fraction possessing similar fluctuations to the intermittent regime from the present experiments, the gas distribution shows that the bubbles contained in the pipe do not occupy the majority of the cross section and are not the classic Taylor bubbles associated with slug flows in smaller pipes.

Pressure gradient

If the pressure gradient results in Figure 5 are compared with the void fraction data in Table 2 for intermittent and semiannular flow, an interesting feature is that perturbations in the void fraction are replicated in the pressure gradient. Plots of the ratio of standard deviation/mean of the pressure gradient versus gas superficial velocity given in Figure 6 show that for liquid superficial velocities less than 0.5 m/s, maximum and minimum values are obtained. The signifi-

cance of these changes to flow pattern transitions will be discussed later.

Structure velocity

Cross-correlating the time varying, void fraction obtained from the gamma densitometers placed at 39.67 m (SBGD-4) and 39.17 m (FVWM) from the mixing point yields time delay, from which structure velocity is determined as the distance of separation is known. In addition to the flow being fully developed at this distance, the choice of these densitometers for cross-correlation is further motivated by their small integration times (16 and 20 ms) and close proximity (0.5 m). The axial resolution of the gamma densitometers which is the shortest visible structure is estimated using the relationship below:

$$\text{Axial Resolution} = 2 \times \text{structure velocity} \times \text{integration time} \quad (1)$$

The factor of 2 is based on Nyquist's theorem which means that the highest frequency of structures that can be observed is half the sampling frequency. Figure 7 shows that structures from ~ 1 -pipe-diameter in length are resolved by the densitometers used in the present cross correlation analysis.

In Figure 8, typical cross correlation sequences are given for an experiment where there is a distinct time delay and another for which there is no correlation. The structure velocities obtained are compared with the correlation by Nicklin et al.³⁶ for fully developed slug flow in Figure 9. Generally, the agreement is good at 20 and 90 bar for low to medium mixture velocities. The good agreement of the present data with Nicklin et al.³⁶ at low to medium mixture velocities cannot be used to support the existence of slugs as Azzopardi³⁷ has shown that this relationship agrees well with the velocities of void waves in bubbly flow and wispy annular flow. At high mixture velocities, corresponding to high gas velocities, there is no dominant time delay and the experimental structure velocities are indeterminate. The circumferential localization of waves in annular flow observed in large diameter pipes as explained by Azzopardi³⁸ provides an explanation for the cases where there is poor correlation. For

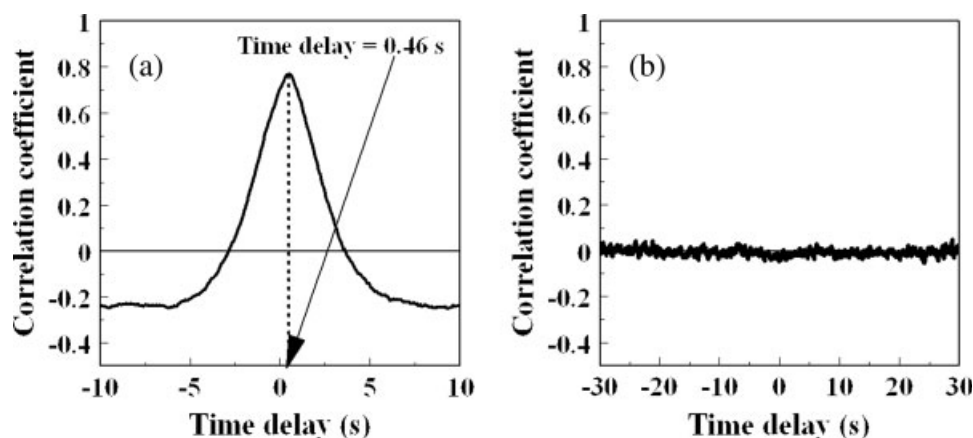


Figure 8. Cross correlation sequence at 20 bar for liquid superficial velocity of 0.05 m/s and gas superficial velocities of: (a) 0.3 m/s; (b) 4.0 m/s.

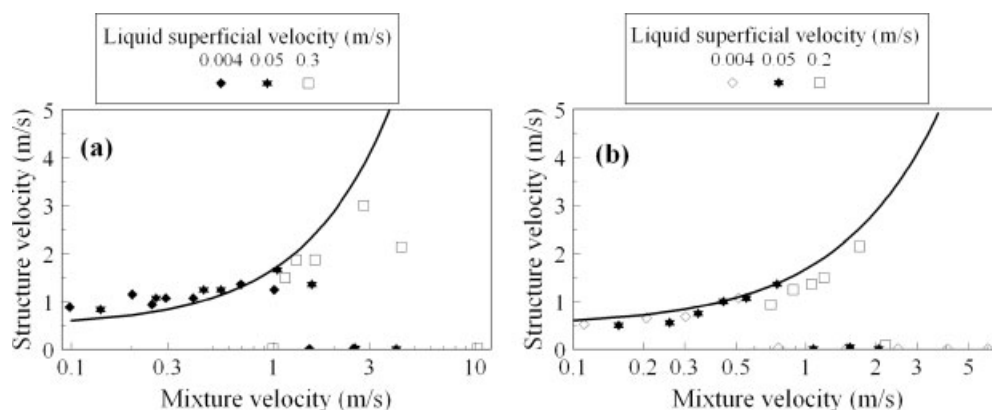


Figure 9. Correlating structure velocity with the relationship of Nicklin et al.³⁶ at: (a) 20 bar; (b) 90 bar.

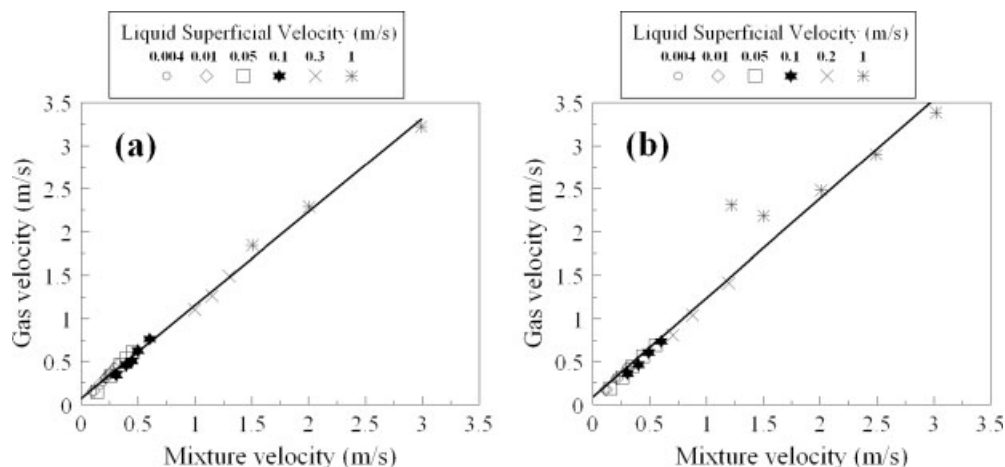


Figure 10. Drift flux relationship at: (a) 20 bar; (b) 90 bar.

liquid superficial velocities than 1 and 0.5 m/s at 20 and 90 bar, respectively, the time varying, void fraction data do not show any strong correlation due to the absence of any pronounced structures and the dispersed nature of the flow.

Drift flux, void fraction, and phase distribution

Zuber and Findlay³⁹ proposed the two-phase flow drift flux model as:

$$U_g = \frac{U_{gs}}{\varepsilon_g} = C_0(U_m) + V_{gd} \quad (2)$$

where U_g , U_{gs} , ε_g , C_0 , U_m , and V_{gd} are gas velocity, gas superficial velocity, void fraction, distribution coefficient, mixture velocity, and drift velocity, respectively.

Table 3. Comparison of Drift Flux Parameters with Kataoka and Ishii (1987)⁴⁰

		Present Data	Kataoka and Ishii (1987)
20 bar	Drift velocity, m/s	0.07	0.19
	Distribution coefficient	1.08	1.16
90 bar	Drift velocity, m/s	0.09	0.13
	Distribution coefficient	1.15	1.12

ture velocity, and drift velocity, respectively. Figure 10 shows that for the present data, a linear relationship exists between the gas and mixture velocities. The drift velocity and distribution coefficient which are given by the slope and y-intercept respectively, are presented in Table 3 along with the

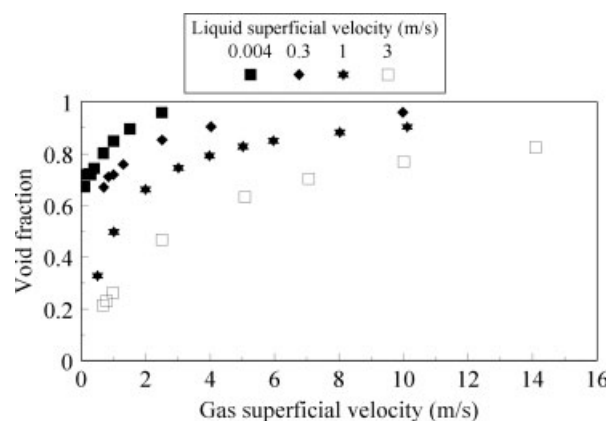


Figure 11. Effect of gas and liquid superficial velocities on void fraction.

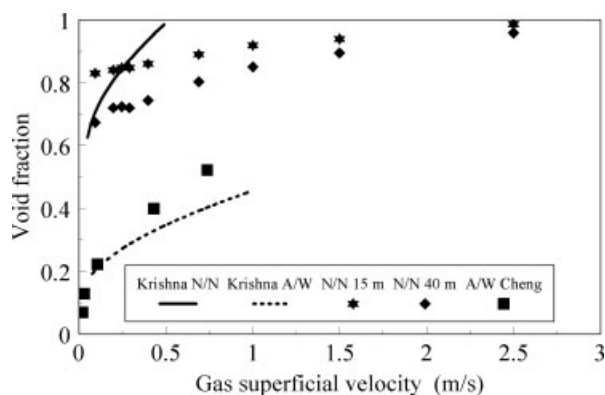


Figure 12. Comparison of measured void fraction with model of Krishna et al.¹⁸

N/N—nitrogen/naphtha, present work at 15 or 40 m from entrance. Liquid superficial velocity = 0.004 m/s. A/W—air/water data from Cheng et al.⁴—pipe diameter = 150 mm—liquid superficial velocity = 0 m/s.

predictions from Kataoka and Ishii.⁴⁰ The correlation of Kataoka and Ishii⁴⁰ overpredicts the drift velocities at 20 and 90 bar, but is consistent with the distribution coefficient. Shoukri et al.⁴¹ applied the drift flux relationship to their air/water data in a 200-mm diameter vertical pipe and that of Hills⁴² for the same mixture in a 150-mm diameter vertical pipe. The drift velocity which is reported to be 0.45 m/s is much greater than the present values of 0.07 and 0.09 m/s at 20 and 90 bar, respectively.

An explanation for this might be found if the void fractions are examined directly. Figure 11 shows data from the 20-bar experiments. Very high void fractions are seen at the lowest liquid flow rate with values decreasing with increasing liquid superficial velocity. The data at the lowest liquid velocity, together with a set from the air/water experiments of Cheng et al.⁴ at zero liquid flow rate, are compared with the model of Letzel et al.¹⁷ in Figure 12. There is good agreement with the data of Cheng et al.⁴ in both gradient and

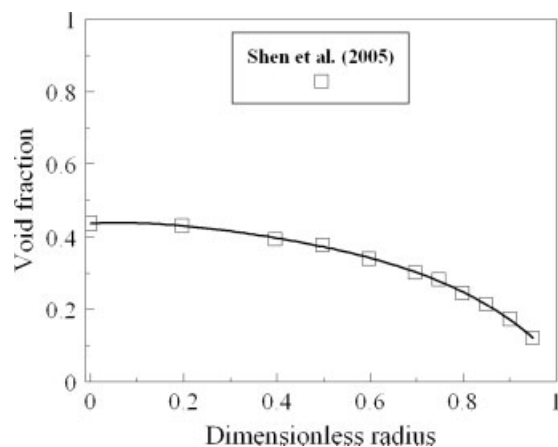


Figure 13. Radial void fraction profile from Shen et al.⁴³ for vertical air/water flow in a 200-mm diameter pipe.

$U_{GS} = 0.372 \text{ m/s}$ and $U_{LS} = 0.072 \text{ m/s}$.

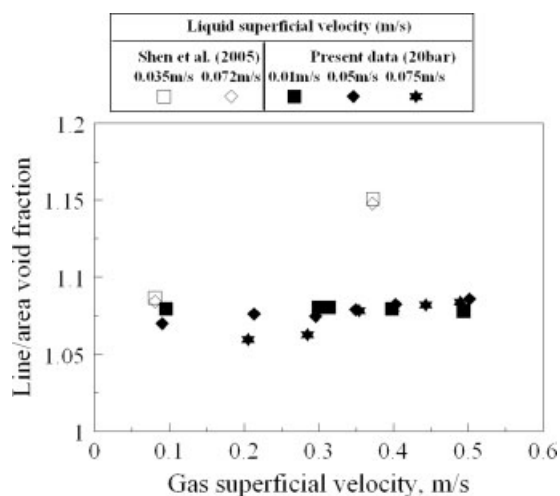


Figure 14. Ratio of line to area void fraction.

absolute values. In the case of the present data the predicted absolute values are approximately correct. However, there is significant difference in the gradients with the experiment

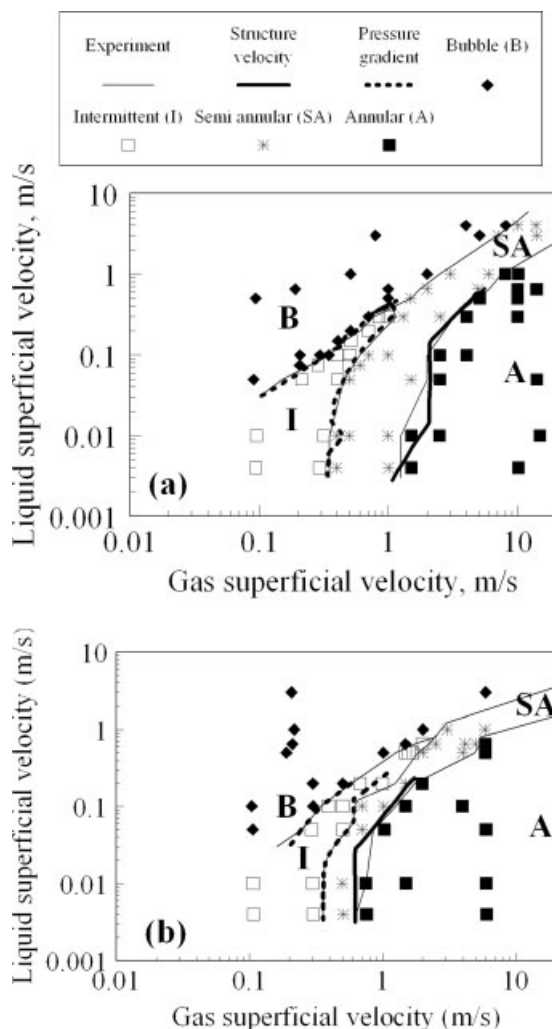


Figure 15. Flow pattern transitions at: (a) 20 bar; (b) 90 bar.

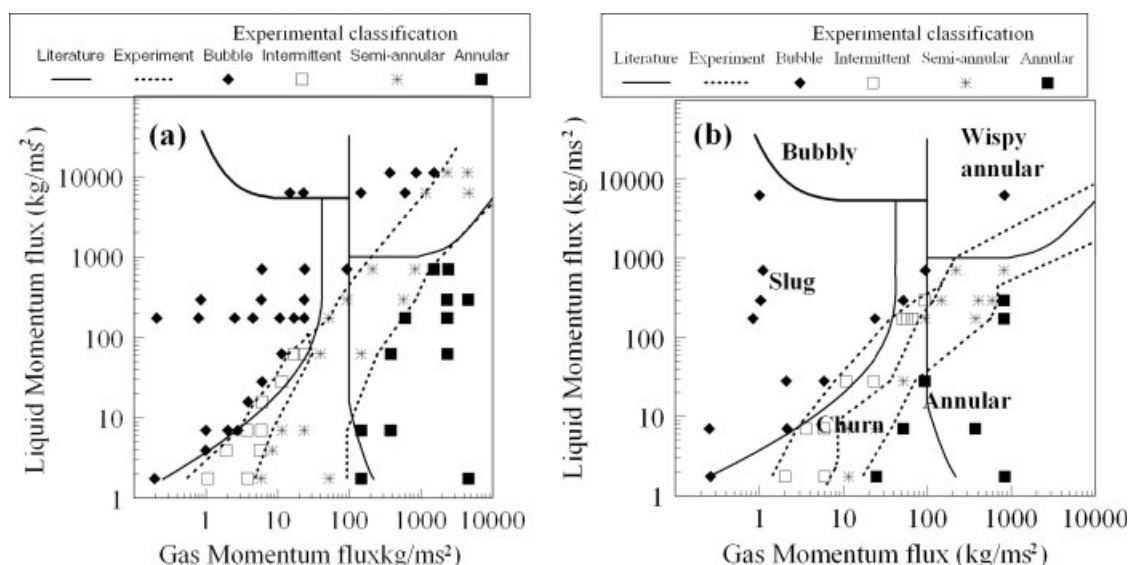


Figure 16. Comparing experimental flow pattern transitions with the Hewitt and Roberts⁴⁴ map at: (a) 20 bar; (b) 90 bar.

gradient being noticeably lower than that of the model. Krishna et al.¹⁸ showed that the effect of increased gas density and that of the presence of additives both give roughly the same increase in void fraction. However, the higher gas density data had a higher gradient than did that for additives. As the present data is for gas density above atmospheric with a liquid which is a mixture of chemicals, the observed high void fractions are probably caused by the two effects. However, the gradient being shallower than that of the model of Letzel et al.¹⁷ (which embodies the gas density effect) suggests that it might be the presence of a mixture of chemicals which is more important. Naphtha being a mixture of chemicals, therefore, explains the high void fraction observed in the present bubble and intermittent flow cases which are in sharp contrast to the much lower values observed in Fig-

ure 4 for two-phase flow involving a pure liquid, that is, water.

Ratios of mean line to mean area void fraction for the data presented here have been compared with the equivalent information from the work of Shen et al.⁴³ Line and area void fractions are obtained from SBGD-5 and the FVWM, respectively in the present work. Shen et al.⁴³ gives the area void fraction directly. For line void fraction, the equation of the best fit curve through the local data from different radial positions is used to determine radial void fraction profile. The average is taken as the mean line void fraction (Figure 13). Figure 14 shows that the present line/area void fraction ratios are similar to Shen et al.⁴³ at a gas velocity of 0.1 m/s, but diverge at higher gas velocities. This suggests differences in the void fraction profiles for both datasets.

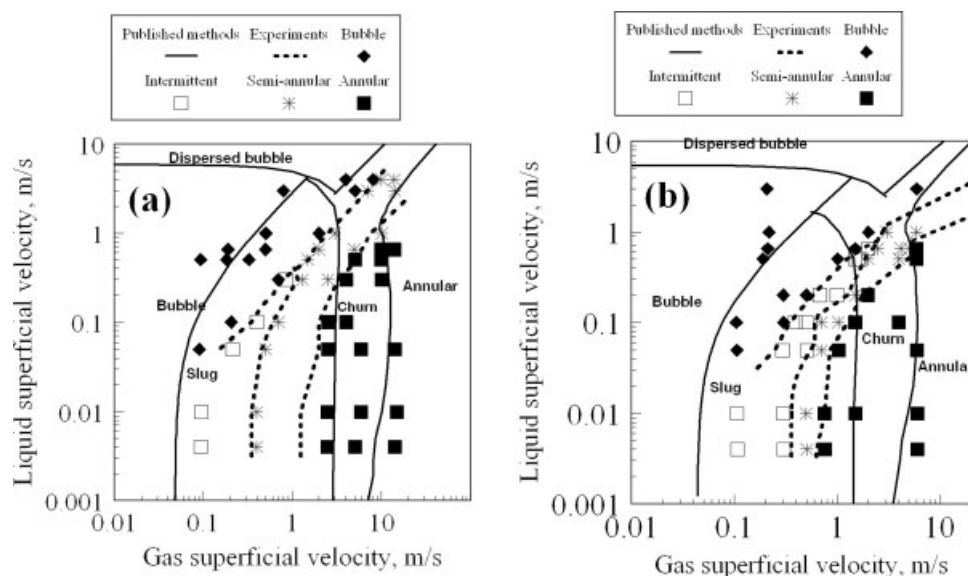


Figure 17. Comparing experimental flow pattern transitions with published methods at: (a) 20 bar; (b) 90 bar.

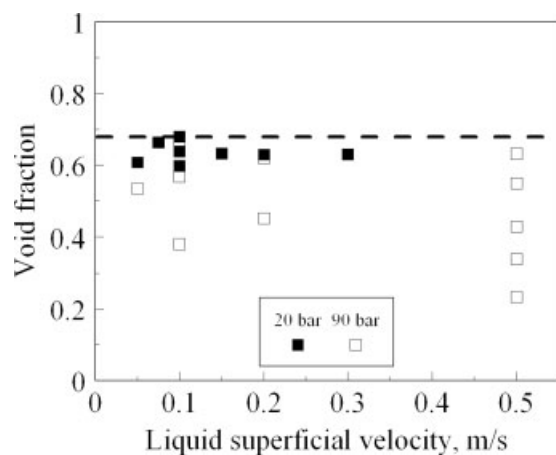


Figure 18. Mean void fraction for bubble flow from the present experiments.

Flow Pattern Transitions

Figure 15 shows the flow pattern transitions for the present experiments at 20 and 90 bar using time varying, void fraction, and their PDF distributions. The major effect of pressure is the reduced semiannular flow region at 90 bar in comparison with 20 bar. Interestingly, the deviation of the structure velocity from the correlation of Nicklin et al.³⁶ agrees well with the transition from semiannular to annular flow. This follows on from Omebere-Iyari and Azzopardi³⁵ who successfully used the changes in structure velocity to delineate flow pattern transition in a 5-mm pipe. Furthermore, the maximum and minimum values in the ratio of standard deviation to the mean of pressure gradient versus gas superficial velocity as shown in Figure 6, coincide with the onset of intermittent and semiannular flows, respectively.

Two gradations of flow pattern maps of varying complexities have been compared with the present experiments. The first level is the map of Hewitt and Robert,⁴⁴ which was derived using data for air/water at 3 bar and steam/water at 35 and 70 bar. Figure 16 shows that the Hewitt and Roberts map is in poor

agreement with the present flow pattern transitions at both 20 and 90 bar. This is attributed to its empirical nature.

The second level flow map pattern encompasses the bubble-to-slug, bubble-to-dispersed bubble, and the dispersed bubble-to-intermittent flow transitions of Taitel et al.,⁵ the slug-to-churn transition by Jayanti and Hewitt²² and the annular-to-intermittent flow transition from Barnea.³¹ This map is compared with the present experiments in Figure 17. The agreement with the present experiments is still very poor. Hence, some of the most commonly used methods from the literature fail to correctly predict any of the flow pattern transitions observed in the present experiments. This implies that the flow pattern models which form the basis of these correlations are not applicable to nitrogen-naphtha flows in large diameter risers at high pressures.

A modification to the bubble/slug transition of Taitel⁵ is made by adjusting the critical voidage to 0.68, which is the maximum value observed for the present bubble flow data (Figure 18). This agrees well with the transition to intermittent flow based on PDF plots as shown in Figure 19.

Conclusions

From the above, the following conclusions can be drawn:

1. The flow patterns observed in a 189-mm diameter vertical pipe are remarkably different to the established ones based on experiments in smaller pipes.
2. Slug flow, as defined for vertical two-phase flow systems to consist of a Taylor bubble occupying the whole pipe cross section and a liquid slug body, is absent.
3. The experimental drift velocity is lower than that reported by Shoukri et al.⁴¹ (using an air/water mixture in a similar-sized pipe) and the predictions of Kataoka and Ishii.⁴⁰ However, examination of data from bubble columns indicates that the difference might be due to the liquid being a mixture of chemicals. This influences the bubble sizes and hence the void fraction.
4. A test of some of the published methods for flow pattern transitions available in the literature gives poor results for high pressure naphtha/nitrogen flow in a large diameter

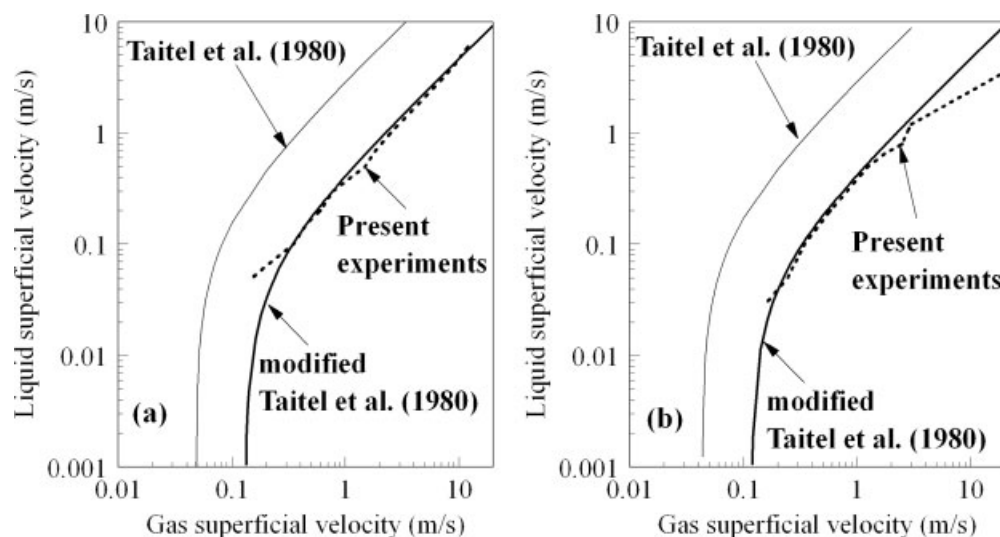


Figure 19. Comparing the bubble/slug transition of Taitel et al.⁵ with the present experiments at: (a) 20 bar; (b) 90 bar.

pipe. However, a modification to the bubble/slug transition of Taitel et al.⁵ gives good agreement.

5. Maxima and minima in the ratio of standard deviation of pressure gradient to the mean values of that parameter and in structure velocity provide a novel method for delineating flow pattern transitions.

Acknowledgments

This work has been undertaken within the Joint Project on Transient Multiphase Flows. The Authors wish to acknowledge the contributions made to this project by the Engineering and Physical Sciences Research Council (EPSRC), the Department of Trade and Industry and the following: Advantica; AspenTech; BP Exploration; Chevron; ConocoPhillips; ENI; ExxonMobil; FEESA; Granherne / Subsea 7; Institutt for Energiteknikk; Institut Français du Pétrole; Norsk Hydro; Petrobras, Scandpower; Shell; SINTEF; Statoil and TOTAL. The Authors wish to express their sincere gratitude for this support.

The experimental programme at SINTEF, Trondheim was made possible by the funded EU programme "Access to Research Infrastructures."

Literature Cited

- Hills JH. The operation of a bubble column at high throughputs: I. gas hold-up measurements. *Chem Eng J*. 1976;12:89–99.
- Hashemi A, Kim JH, Sursack JP. Effect of diameter and geometry on two-phase flow regimes and carry-over in a model PWR hot leg. *Proc 8th Int Heat Transfer Conf*. 1986;5:2443–2451.
- Kytomaa HK, Brennen CE. Small amplitude kinematic wave propagation in two-component media. *Int J Multiphase Flow*. 1991;17:13–26.
- Cheng H, Hills JH, Azzopardi BJ. A study of the bubble to slug transition in vertical gas-liquid flow in columns of different diameter. *Int J Multiphase Flow*. 1998;24:431–452.
- Taitel Y, Barnea D, Dukler AE. Modelling flow pattern transitions for steady upward gas-liquid flow in vertical tubes. *AIChE J*. 1980;26:345–354.
- Costigan G, Whalley PB. Slug flow regime identification from dynamic void fraction measurements in vertical air-water flows. *Int J Multiphase Flow*. 1997;23:263–282.
- Ohnuki A, Akimoto H. Experimental study on transition of flow pattern and phase distribution in upward air-water two-phase flow along a large vertical pipe. *Int J Multiphase Flow*. 2000;26:267–286.
- Prasser HM, Beyer M, Bottger A, Carl H, Lucas D, Schaffrath A, Schutz P, Weiss FP, Zschau J. Influence of the pipe diameter on the structure of the gas-liquid interface in a vertical two-phase pipe flow. *10th Int Topical Meeting on Nuclear Reactor Thermal Hydraulics (NURETH-10)*, Seoul, South Korea, October, 2003.
- Kobayashi A, Shakutsui H, Mitsuyoshi M, Minagawa H. Void fraction in upward gas-liquid two-phase flow in a large diameter pipe. *5th Int Conf Multiphase Flow*, Yokohama, Japan, May–June, 2004.
- Hibiki T, Ishii M. Experimental study on hot-leg U-bend two-phase natural circulation in a loop with a large diameter pipe. *Nucl Eng Des*. 2000;195:69–84.
- Shoukri M, Hassan I, Gerges IE. Two-phase bubbly flow structure in large-diameter vertical pipes. *Can J Chem Eng*. 2003;81:205–211.
- Zhu W, Ching C, Shoukri M. Phase distribution and flow regime transition of two-phase flow in large diameter pipes. *5th Int Conf Multiphase Flow*, Yokohama, Japan, May 30–June 4 2004.
- Hills JH, Cheng H, Azzopardi BJ. Void fraction waves in vertical gas-liquid flow in a 150 mm tube. *3rd Int Conf Multiphase Flow*, Lyon, France, 8–12 June 1998.
- Krishna R, Ellenberger J. Gas holdup in bubble column reactors operating in the churn-turbulent regime. *AIChE J*. 1996;42:2627–2634.
- Chaumat H, Billet-Duquenne AM, Augier F, Methieu C, Delmas H. Mass transfer in bubble column for industrial conditions—effects of organic medium, gas and liquid flow rates and column design. *Chem Eng Sci*. 2005;60:5930–5936.
- Fan L-S, Yang CQ, Lee DJ, Tsuchiya K, Luo X. Some aspects of high-pressure phenomena of bubbles in liquids and liquid-solid suspensions. *Chem Eng Sci*. 1999;54:4681–4709.
- Letzel HM, Schouten JC, Krishna R, van den Bleek CM. Gas holdup and mass transfer in bubble column reactors operated at elevated pressure. *Chem Eng Sci*. 1999;54:2237–2246.
- Krishna R, Urseanu MI, Dreher AJ. Gas hold-up in bubble columns: influence of alcohol addition versus operation at elevated pressures. *Chem Eng Proc*. 2000;39:371–378.
- Camarasa E, Vial C, Poncin S, Wild G, Midoux N, Bouillard J. Influence of coalescence behavior of the liquid and of gas sparging on hydrodynamics and bubble characteristics in a bubble column. *Chem Eng Proc*. 1999;38:329–344.
- Shäfer R, Merten C, Eigenberger G. Bubble size distributions in a bubble column reactor under industrial conditions. *Exp Therm Fluid Sci*. 2002;26:595–604.
- Radovich NA, Moissis R. The transition from two-phase bubble flow to slug flow. MIT Report 7-7673-22, 1962.
- Jayanti S, Hewitt GF. Prediction of the slug-to-churn flow transition in vertical two-phase flow. *Int J Multiphase Flow*. 1992;18:847–860.
- Dukler AE, Taitel Y. Flow pattern transitions in gas-liquid systems: measurement and modelling. *Multiphase Sci Tech*. 1986;2:53–57.
- McQuillan KW, Whalley PB. Flow patterns in vertical two-phase flow. *Int J Multiphase Flow*. 1985;11:161–175.
- Mishima K, Ishii M. Flow regime transition criteria for upward two-phase flow in vertical tubes. *Int J Heat Mass Trans*. 1984;27:723–737.
- Brauner N, Barnea D. Slug/churn transition in upward gas-liquid flow. *Chem Eng Sci*. 1986;41:159–163.
- Brotz W. Über die vorausberechnung der absorptionsgeschwindigkeit con gasen in stromenden flüssigkeitsschichten. *Chem Ing Tech*. 1954;26:470.
- Fulford GD. The flow of liquid in thin films. *Adv Chem Eng*. 1964;5:151–236.
- Nusselt W. Surface condensation of water. *Z Ver Ing*. 1916;60:541–546, 569–575.
- Watson MJ, Hewitt GF. Pressure effects on the slug to churn transition. *Int J Multiphase Flow*. 1999;25:1225–1241.
- Barnea D. Transition from annular flow and from dispersed bubble flow—unified models for the whole range of pipe inclinations. *Int J Multiphase Flow*. 1986;12:733–744.
- Barnea D. A unified model for predicting flow-pattern transitions for the whole range of pipe inclinations. *Int J Multiphase Flow*. 1987;13:1–12.
- Norris HL III, Fuchs P, Malnes D, Klemp S. Developments in the simulation and design of multiphase pipeline systems. *60th Annual Tech Conf SPE*, Las Vegas, USA, June 1985.
- Azzopardi BJ. Gas-Liquid Flows. New York: Begell House, 2006.
- Omebere-Iyari NK, Azzopardi BJ. A study of flow patterns for gas/liquid flow in small diameter tubes. *Chem Eng Res Des*. 2007;85:180–192.
- Nicklin DJ, Wilkes JO, Davidson JF. Two-phase flow in vertical tubes. *Trans Inst Chem Eng*. 1962;40:61–68.
- Azzopardi BJ. Bubbles, drops and waves: differences or underlying commonality. *42nd European Two-Phase Flow Group Meeting*, Genoa, 23–25 June, 2004.
- Azzopardi BJ. Drops in annular two-phase flow. *Int J Multiphase Flow*. 1997;23:1–53.
- Zuber N, Findlay JA. Average volumetric concentration in two-phase flow systems. *J Heat Trans*. 1965;87:453–468.
- Kataoka I, Ishii M. Drift flux model for large diameter pipe and new correlation for pool void fraction. *Int J Heat Mass Trans*. 1987;30:1927–1939.
- Shoukri M, Stankovic B, Hassan I, Dimmick J. Effect of pipe diameter on flow pattern transitions and void fraction of air-water flow in vertical pipes. *8th Int Conf Nuclear Eng*, Baltimore, USA, 2000.
- Hills JH. The behavior of a bubble column at high throughputs: II. Radial voidage profiles. *Chem Eng J*. 1993;53:115–123.
- Shen X, Mishima K, Nakamura H. Two-phase phase distribution in a vertical large diameter pipe. *Int J Heat Mass Trans*. 2005;48:211–225.
- Hewitt GF, Roberts DN. Studies of two-phase flow patterns by simultaneous X-rays and flash photography. Atomic Energy Research Establishment Harwell, England. Report M-2159, 1969.

Manuscript received Aug. 24, 2007, and revision received July 5, 2007